♦ ISEV

RESEARCH ARTICLE

Profile of matrix-entrapped extracellular vesicles of microenvironmental and infiltrating cell origin in decellularized colorectal cancer and adjacent mucosa

Sarah Tassinari[1] | Edoardo D'Angelo[2,3] | Federico Caicci[4] | Cristina Grange[5] |
Jacopo Burrello[5] | Matteo Fassan[6,7] | Alessia Brossa[1] 🆔 | Riccardo Quoc Bao[2] |
Gaya Spolverato[2] | Marco Agostini[2,3] | Federica Collino[8,9,10,*] 🆔 | Benedetta Bussolati[1,*] 🆔

[1]Department of Molecular Biotechnology and Health Sciences, University of Torino, Torino, Italy

[2]General Surgery 3, Department of Surgery, Oncology and Gastroenterology, University of Padova, Padua, Italy

[3]NanoInspired biomedicine lab, Fondazione Istituto di Ricerca Pediatrica Città della Speranza, Padua, Italy

[4]Department of Biology, University of Padova, Padua, Italy

[5]Department of Medical Science, University of Torino, Torino, Italy

[6]Department of Medicine (DIMED), University of Padua, Padua, Italy

[7]Veneto Institute of Oncology IOV - IRCCS, Padua, Italy

[8]Laboratory of Translational Research in Paediatric Nephro-Urology, Fondazione IRCCS Ca' Granda Ospedale Maggiore Policlinico, Milano, Italy

[9]Pediatric Nephrology, Dialysis and Transplant Unit, Fondazione IRCCS Ca' Granda Ospedale Maggiore Policlinico, Milano, Italy

[10]Department of Clinical Sciences and Community Health, University of Milano, Milan, Italy

Correspondence
Benedetta Bussolati, Molecular Biotechnology Center, University of Turin, via Nizza 52, 10126 Turin, Italy. Email: benedetta.bussolati@unito.it

Abstract

Cellular elements that infiltrate and surround tumours and pre-metastatic tissues have a prominent role in tumour invasion and growth. The extracellular vesicles specifically entrapped and stored within the extracellular matrix (ECM-EVs) may reflect the different populations of the tumour microenvironment and their change during tumour progression. However, their profile is at present unknown. To elucidate this aspect, we isolated and characterized EVs from decellularized surgical specimens of colorectal cancer and adjacent colon mucosa and analyzed their surface marker profile. ECM-EVs in tumours and surrounding mucosa mainly expressed markers of lymphocytes, natural killer cells, antigen-presenting cells, and platelets, as well as epithelial cells, representing a multicellular microenvironment. No difference in surface marker expression was observed between tumour and mucosa ECM-EVs in stage II-III tumours. At variance, in the colon mucosa adjacent to stage IV carcinomas, ECM-EV profile showed a significantly increased level of immune, epithelial and platelet markers in comparison to the matrix of the corresponding tumour. The increase of EVs from immune cells and platelets was not observed in the mucosa adjacent to low-stage tumours. In addition, CD25, a T-lymphocyte marker, resulted specifically overexpressed by ECM-EVs from stage IV carcinomas, possibly

---

*Federica Collino and Benedetta Bussolati equal contribution.

correlated with the pro-tolerogenic environment found in the corresponding tumour tissue. These results outline the tissue microenvironmental profile of EVs in colorectal carcinoma-derived ECM and unveil a profound change in the healthy mucosa adjacent to high-stage tumours.

KEYWORDS
biomarkers, colorectal cancer, decellularized tissues, extracellular matrix, tumour infiltration, tumour invasion, tumour microenvironment

1 | INTRODUCTION

Extracellular vesicles (EVs), phospholipid bilayer-covered particles released by cells into the extracellular space, interact with the surrounding extracellular matrix (ECM) where they can be trapped, or navigate through it toward biological fluids for long-distance communication (van Niel et al., 2018). Likewise, circulating EVs reaching target organs can be stored in the ECM once they extravasate, resulting in their increased lifespan and long-term effects (van Niel et al., 2018). Electron microscopy studies clearly showed the presence of EVs in the extracellular space, in normal and tumour tissue (Crescitelli et al., 2021). In fact, EVs are nowadays considered a functional component of the ECM (Rilla et al., 2019), and increasing interest is directed toward the specific phenotypic and functional characterization of the ECM-EVs.

ECM-EVs have been previously isolated from normal tissues, including derma, bladder, and intestinal mucosa (Huleihel et al., 2016) after decellularization, a strategy allowing cell removal without or minimally affecting ECM composition (Piccoli et al., 2018). In that study, intact ECM-EVs were detected in tissue-derived scaffolds (both commercial and freshly prepared from decellularized tissues) and characterized to express ECM component ligands on their surface and a miRNA cargo relevant for scaffold application for regenerative medicine (Huleihel et al., 2016). Indeed, it is well known that the decellularization step does not alter the distribution of ECM-proteins or the matrix-bound growth factors (D'Angelo et al., 2020; Piccoli et al., 2018). On the other hand, little information is present on EVs retained within the matrix in tumours. In fact, tumour-derived EVs have been only isolated through digestion of the entire and fresh tissue. This is a procedure that does not allow to distinguish the ECM-EVs from the tissue-derived EVs, that also include EVs in the interstitial space between cells, or adjacent to cells, or directly derived from cells during the isolation process (Crescitelli et al., 2021).

Different cellular components are part of the tumour microenvironment and co-evolve with cancer, including fibroblasts, endothelial cells and blood-derived infiltrating cells, such as myeloid cells, lymphocytes and platelets (Cheng et al., 2013; Cirri & Chiarugi, 2011; Gabrilovich et al., 2012). As EV surface markers reflect the originating cells, the characterization of EVs within ECM could elucidate the composition of the tumour microenvironment and on its changes during tumour progression. We believe that the analysis of the different EV subpopulations within tumour ECM and surrounding non-infiltrated mucosa may provide a signature of the different populations representing the tumour microenvironment and of their possible interactions.

In the present study, we therefore isolated and characterized EVs from 23 colorectal cancer decellularized surgical specimens (CRC-ECM-EVs), at different tumour stages, and analyzed the surface profile composition, in comparison with that of healthy colon decellularized mucosa (HC-ECM-EVs) from the same patient. In particular, using the MACSPlex kit, we profiled EVs for markers of tumour microenvironment and immune cells. ECM-EVs in tumour tissue expressed immune, platelet as well as epithelial cell markers. The levels of markers of immune cells and platelets, possibly infiltrating the tissue and entrapped within ECM, significantly increased in ECM-EVs of healthy mucosa adjacent to stage IV tumours, compared to the tumour matrix. Moreover, CD25, a T-lymphocyte marker, was specifically increased in CRC-ECM-EVs from stage IV tumour with respect to both the lower stage tumour and the surrounding healthy mucosa.

2 | MATERIALS AND METHODS

2.1 | Patients and consent

ECM has been obtained by the decellularization of human colorectal cancer biopsy and normal colon biopsy as control. Tissue samples from CRC patients who underwent curative surgery between February 2015 and December 2021 were collected from Tissue biobank of the General Surgery 3 (University-Hospital of Padova). A total of 23 primary colon tumour biopsies and the corresponding normal colon mucosa were processed to isolate EVs for different analyses. CRC tissues were obtained at the edge of infiltrating neoplasia while healthy colon mucosa was obtained at least 10 cm far from the cancer lesion.

TABLE 1 Clinical-pathological characteristics of CRC patients enrolled in the study (II-III stage: $N = 11$, IV stage: $n = 12$).

Patient	Sex	Age	T	N	M	TNM	G
01	M	82	4a	1b	1b	4b	2
02	F	76	3	1b	1a	4a	2/3
03	M	69	3	2b	1a	4a	2/3
04	M	54	4a	2b	0	3c	3
05	M	81	4a	1a	0	3b	2
06	F	85	3	0	0	2a	2
07	F	84	3	0	0	2a	1
08	F	75	3	0	0	2a	3
09	F	75	3	0	0	2a	2
10	F	85	3	0	0	2a	2
11	F	76	3	0	0	2a	2
12	M	82	3	0	0	2a	2
13	M	59	4b	0	0	2b	2
14	M	47	3	2a	1c	4c	3
15	M	79	4a	2b	1a	4a	3
16	F	55	3	2a	1a	4a	3
17	M	63	4a	1a	1c	4c	3
18	M	80	3	1b	1a	4a	2
19	F	80	3	2a	1a	4a	3
20	F	63	4a	1b	1a	4a	3
21	F	52	3	1b	1c	4c	3
22	F	83	3	1b	1a	4a	2/3
23	M	76	3	2	0	3b	3

Abbreviations: T: Tumour; N: Node; M: Metastasis; TNM: Tumour Node Metastasis stage; G: Grade. TNM was defined according to the 8th edition of the AJCC/UICC TNM staging system.

This study was conducted according to the principles expressed in the Declaration of Helsinki. Written informed consent was obtained from every enrolled individual and protocol was approved by ethics committee of institution (Ethical Committee Approved Protocol Number: 448/2002). All the patients enrolled fulfilled the following inclusion criteria: histologically confirmed primary adenocarcinoma of the colon, age of more than 18 years, and written informed consent. Patients with a known history of hereditary colorectal cancer syndrome and patients that underwent neoadjuvant treatments were excluded. Patients' clinical and pathological characteristics are summarized in Table 1.

2.2 | EV extraction from decellularized CRC and HC biopsies

Tissue decellularization process was performed using an established protocol based on two detergent-enzymatic treatment cycles, as previously described (Piccoli et al., 2018). All decellularized samples were frozen after the decellularization process (D'Angelo et al., 2020) The decellularized matrix underwent enzymatic digestion to allow the detachment of the EVs. Collagenase and Proteinase K (both 1 mg/mL in RPMI), affecting different membrane components, were tested. The Proteinase K treatment showed the best results as the number of EV recovered/integrity. Briefly, decellularized tissues were weighed, cut into small pieces, and then digested for 40 min at 37°C under constant shaking. After incubation, the digested pieces were kept on ice to inactivate the enzyme and then transferred into a 40 μm pore size (BD Falcon, NJ) cell strainer and washed with 5 mL PBS to permit EV release. The filtered solution was subjected to differential centrifugation and the supernatant was finally ultracentrifuged at 100,000 $\times$ g (Beckman Coulter Optima L-90K ultracentrifuge; Beckman Coulter, CA) for 2 h at 4°C using a type 70ti rotor. Collected EVs were then resuspended in serum-free RPMI-1640 supplemented with 1% DMSO and stored at −80°C. A schematic representation of the extraction protocol is reported in Figure 1a. EVs were also extracted from the fresh tissue before decellularization ($n = 5$), following the protocol described by Crescitelli et al. (2021).
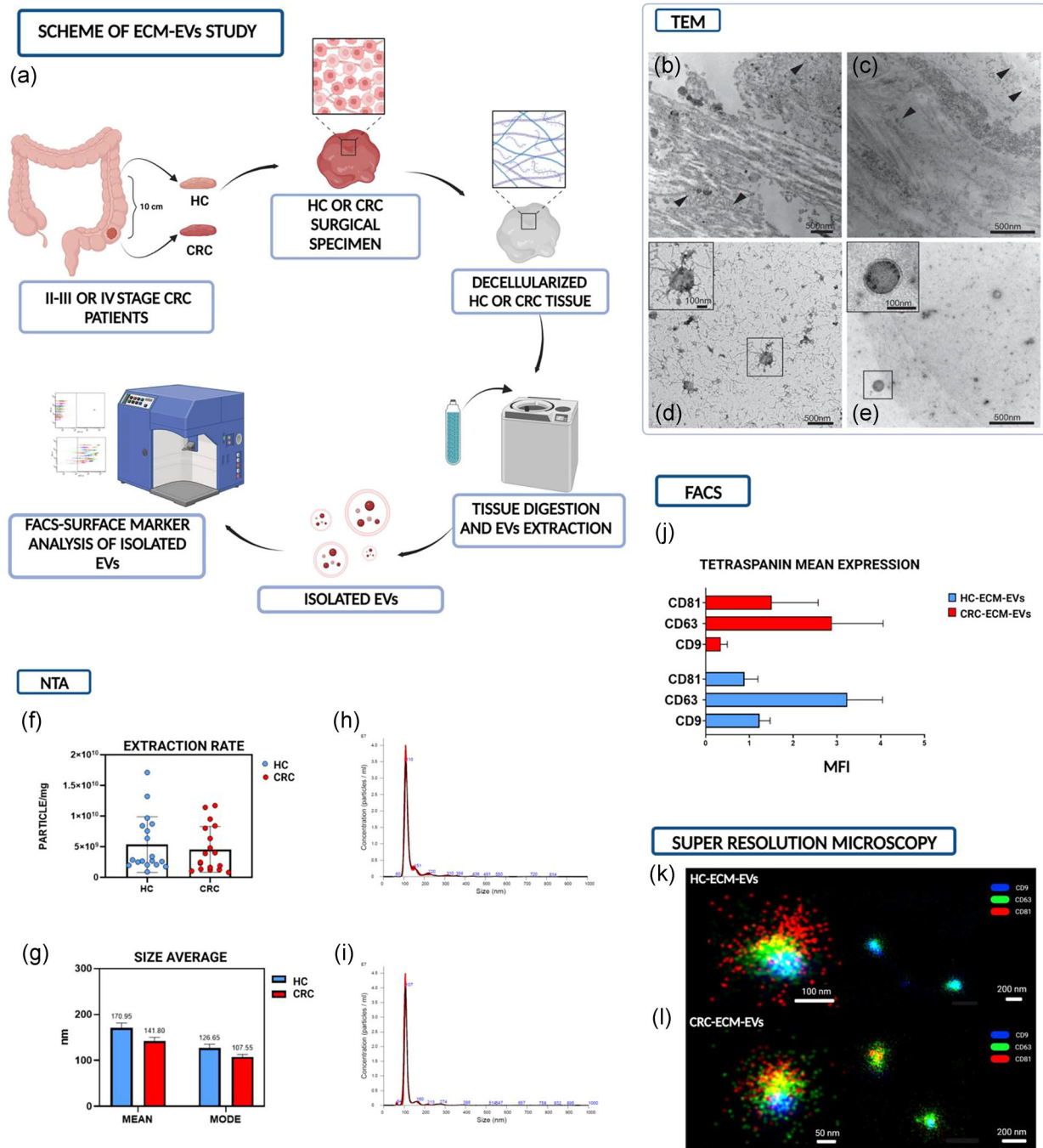
FIGURE 1 ECM-EV extraction from tumour and healthy mucosa and their characterization. (a) Schematic representation of the study. (b-c) TEM images of EVs trapped in healthy (HC-ECM-EVs, b) and tumour (CRC-ECM-EVs, c) decellularized tissues. (d-e) TEM images of CRC-ECM-EVs extracted with Collagenase (d) and Proteinase K (e). (f-g) Concentration of EVs extracted from decellularized healthy (f) and tumour tissues (g) and their size distribution. (h-i) Representative NTA analysis of HC-ECM-EVs (h) and CRC-ECM-EVs (i). (j) Tetraspanin mean expression in ECM-EVs of all samples in the study ($n = 23$) quantified via bead-based flow cytometry using MACSPlex assay. MFI: mean fluorescence intensity. (k-l) Representative super-resolution images of triple (left) and double (right) tetraspanins positive ECM-EVs.

2.3 | Immunohistochemistry

Formalin-fixed paraffin sections (8 μm) from II-III and IV stage CRC ($n = 3$ patients/stage) were stained using the following antibodies (clone, dilution, manufacturer): CD4 (clone CD4/4B12, 1:100, Dako, Santa Clara, CA), FOXP3 (clone 236A/E7, 1:100 Abcam, Cambridge, UK) and CD25 (clone BC96, 1:100, Santa Cruz Biotechnology, Dallas, TX). Immunohistochemistry staining was automatically performed using the Bond Polymer Refine Detection kit (Leica Biosystems, Wetzlar, Germany) in the

BOND-MAX system (Leica Biosystems). The expression of FOXP3^{+} and CD25^{+} cells was scored in sequential sections according to the percent of positive lymphocytes in the tumour and in the invasive margin and quantified in at least three independent high-power fields magnified at 40X for each patient.

2.4 | Nanoparticle tracking analysis

The concentration and size distribution of EV were determined by Nanoparticle tracking analysis (NTA) using the Nanosight LS300 system (Malvern Panalytical, Malvern, UK) equipped with a 488 nm laser module. Briefly, EVs were diluted (1:100) in a sterile saline solution and analyzed using the NTA 3.2 Analytical Software. Three videos of 60 s at camera level 14 and threshold 3 were captured using a syringe pump 30. The NTA settings were kept constant between samples.

2.5 | Transmission electron microscopy analyses

Transmission electron microscopy (TEM) was performed to characterize the EV structure. Briefly, EVs were placed on a 400-mesh holey film grid and stained with 2% uranyl acetate. The sample was observed with a Tecnai G2 (FEI) transmission electron microscope operating at 100 kV. Images were captured with a Veleta (Olympus Soft Imaging System) digital camera. Moreover, TEM was conducted to investigate the presence of EVs trapped inside the extracellular matrix. The ECM was fixed with 2.5% glutaraldehyde in 0.1 M sodium cacodylate buffer pH 7.4 overnight at 4°C, then postfixed with 1% osmium tetroxide in 0.1 M sodium cacodylate buffer for 1 h at 4°C. After three water washes, ECM was dehydrated in a graded ethanol series and embedded in an epoxy resin (Sigma-Aldrich). Ultrathin sections (60-70 nm) were obtained with an Ultrotome V (LKB) ultramicrotome, counterstained with uranyl acetate and lead citrate, and viewed with a Tecnai G2 (FEI) transmission electron microscope operating at 100 kV.

2.6 | Super-resolution microscopy

Single ECM-EV surface marker analysis was conducted using a temperature-controlled Nanoimager S Mark II microscope from ONI (Oxford Nanoimaging, Oxford, UK) equipped with a 100X, 1.4NA oil immersion objective, an XYZ closed-loop piezo 736 stage, and 405 nm/150 mW, 473 nm/1 W, 560 nm/1 W, 640 nm/1 W lasers, as described (Gebara et al., 2022). EV profiler Kit (ONI) was utilized for the experiments following the manufacturer's protocol. The Kit contains fluorescent antibodies anti CD9-488, CD63-568, and CD81-647. Moreover, antibodies anti CD4-488 and CD25-647 (both from BD Biosciences, Franklin Lakes, New Jersey) were used instead of those present in the EV profiler Kit. dSTORM mode acquired sequentially in total reflection fluorescence (TIRF) mode was used for the acquisition of images (2000 frames for each channel). Before each imaging session, bead slide calibration was performed to align fluorescent channels, achieving a channel mapping precision smaller than 12 nm. Single-molecule data was filtered using NimOS software (v.1.18.3, ONI). Data has been processed with the Collaborative Discovery (CODI) online analysis platform (www.alto.codi.bio) from ONI and the drift correction pipeline version 0.2.3 was used.

2.7 | Cytofluorimetric bead-based analyses

EV surface markers were investigated using a bead-based cytofluorimetric analysis using the human MACSPlex exosome kit (Miltenyi Biotec, Bergisch Gladbach, Germany). Shortly, $1*10^9$ ECM-EVs were diluted with MACSPlex Buffer to a final volume of 120 μL. A total of 15 μL of MACSPlex exosome capture beads (FITC-PE), which contain beads coupled to 37 exosomal surface epitopes and 2 control isotypes, were added to the ECM-EVs that were incubated overnight at 4°C on an orbital shaker (450 rpm) with light protection. The day after, two washing steps were conducted to eliminate unbound EVs and 15 μL of MACSPlex Exosome Detection Reagent cocktail of APC fluorescent antibodies against tetraspanins (CD9, CD63, CD81) were added. The beads-EVs solution was incubated for 1 h at room temperature (RT) with light protection on an orbital shaker (450 rpm). The samples were then washed and incubated at RT, protected from light, on an orbital shaker for 15 min followed by a wash at 3000× g for 5 min. A total of 150 μL of the samples were transferred in flow cytometry tubes and detected using the BD FACSCelesta flow cytometer. The beads-EV solution without the APC-tetraspanins antibodies was used as control. Results were normalized on the mean fluorescence intensity (MFI) for every sample, as previously described (d'Alessandro et al., 2021, Ekström et al., 2022).

2.8 | Statistical analysis

IBM SPSS Statistics 26 (IBM Corp, Armonk, NY) and GraphPad Prism 9 Software (GraphPad Software Inc., La Jolla, CA) were used for analyses and figure preparation. A nonparametric Wilcoxon test (pair or non-pair) was performed to compare CRC and HT samples and CRC at different stages. Receiver Operating Characteristics (ROC) curves were generated for every marker identified using the Univariate statistical analysis to assess the area under the curve (AUC). The AUC was calculated for each significant surface marker identified by the univariate analysis. We only considered AUC values greater than 0.5 for better power performance.

3 | RESULTS

3.1 | EV isolation from healthy- and tumour-derived colorectal decellularized tissue

EVs were extracted from tumour-derived colorectal decellularized biopsies and healthy mucosa, using an enzymatic procedure followed by sequential centrifugations, as shown in Figure 1a. The presence of intact EVs in decellularized colorectal tissue was initially assessed by TEM, that showed EVs trapped both inside the normal and tumour-derived decellularized ECM (Figure 1b-c). When comparing EVs isolated with different enzymatic ECM digestions, TEM analysis showed that EVs extracted using Collagenase treatment retained collagen strengths on their surface, confirming their entrapment in the ECM (Figure 1d). On the contrary, EVs extracted with Proteinase K appeared rounded and completely denudated of ECM residues (Figure 1e). This method was then chosen for further studies. EV size, concentration, and tetraspanins' expression were subsequently assessed. NTA analysis showed no difference in the extraction rate and dimension between healthy and tumour-decellularized tissues (Figure 1f-g). In particular, the recovery yield was $5.35*10^9$ and $4.55*10^9$ particles/mg for preparations extracted from healthy decellularized colon tissue (HC-ECM-EVs) and colorectal cancer decellularized tissue (CRC-ECM-EVs), respectively (Figure 1f). The number of particles, as assessed by NTA, was significantly lower than those isolated from fresh CRC samples containing the cellular components (Supplementary Figure 1). The presence of tetraspanins (CD9, CD63 and CD81) was assessed through bead-based cytofluorimetric analysis using the MACsplex exosome kit and through super-resolution microscopy. CD9, CD63 and CD81 were detected in both HC- and CRC-ECM-EVs, with CD63 showing the highest expression among tetraspanins (Figure 1j). Single vesicle analysis confirmed the homogenous distribution of these molecules on both healthy and colorectal cancer vesicles. Triple, double and single positive EVs were detected for each tetraspanin (Figure 1k-l).

3.2 | ECM-EV surface marker profile in HC and CRC decellularized tissues

The expression of different surface markers on ECM-EVs, mainly related to immune and microenvironmental origin, was assessed using the MACSplex assay, evaluating 37 different surface proteins. Data were normalized to the mean fluorescence intensity of the sample and are reported in Supplementary Table I.

The analysis showed the presence within both normal and tumour ECM-EVs of several immune-derived markers, together with platelet and epithelial markers. In both tumour and healthy mucosa, CD3, CD56, and HLA-DR appeared highly expressed by ECM-EVs, suggesting the entrapment within the matrix of EVs released by T lymphocytes, NK cells, and antigen-presenting cells (Figure 2a,b). Comparing CRC- and HC-ECM-EVs, the ECM-EVs isolated from decellularized normal tissue adjacent to the tumoral lesion (10 cm far) showed a significantly higher expression of CD9, CD40 (costimulatory molecule), CD42a (platelet marker), and CD24 and CD326 (epithelial markers), compared to the tumour counterpart (Figure2c). At variance, no marker was overexpressed in tumour ECM-EVs.

3.3 | ECM-EV profile of healthy mucosa is specifically altered in stage IV patients

Normal and CRC-ECM-EVs were further divided in relation to the tumour stage, in stage II-III ECM-EVs ($n = 11$) and stage IV ECM-EVs ($n = 12$). Interestingly, no significant differences were observed between II-III CRC-ECM-EV and their corresponding HC, indicating that the observed overall differences, shown above in Figure 2, were restricted to stage IV CRC. Indeed, in those samples, the profile of EVs obtained from healthy decellularized colon mucosa showed an overexpression in CD24, CD40, CD42a, and CD326, compared to stage IV decellularized tumour (Figure 3a). In addition, CD44 (adhesion marker) and CD49e (platelet marker), were also increased in the decellularized mucosa compared to stage IV decellularized tumour (Figure 3a). Sensitivity and specificity of the analyzed markers were evaluated by ROC curve analysis, and results were reported in Figure 3b and Supplementary Table 2. The CD49e, CD42a, and CD9 values yielded an AUC above 0.75, separating stage IV tumours from
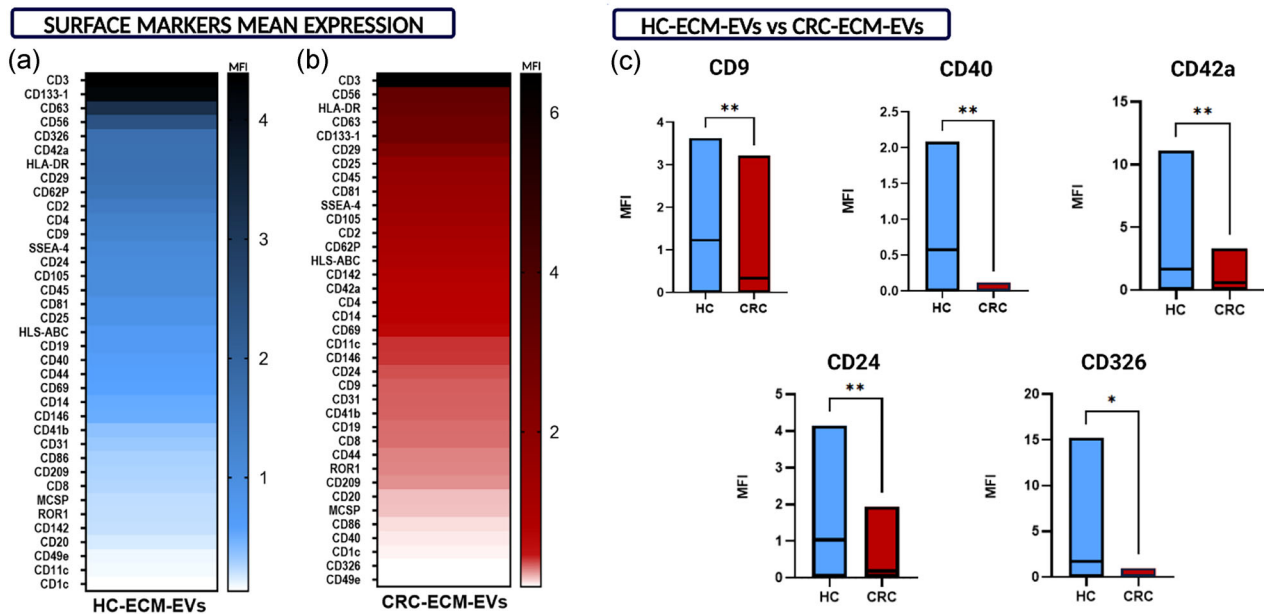
FIGURE 2 Overall comparison of marker expression in HC- and CRC-ECM-EVs. (a-b) Heat map showing the decreasing mean expression intensity of EV markers, applied to EVs extracted from decellularized healthy colon tissue (blue) or colorectal cancer tissue (red). (c) Histogram depicting differentially expressed markers between HC- and CRC-ECM-EVs. Data are expressed as mean fluorescence intensity (MFI). Multiple T-test was performed: *$p < 0.05$, **$p < 0.01$.

non-tumour tissues. These results indicate a specific change in the ECM of the colon mucosa surrounding the tumour that appears restricted to stage IV CRC, with platelet and inflammatory cell infiltration, and possibly activation of epithelial cells.

An increase in platelet (CD42a, CD62p) and epithelial/stem markers (CD326, CD105, SSEA-4, CD44) was also observed when comparing ECM-EVs in mucosa from stage IV CRC in respect to stage II-III CRC (Supplementary Figure 2).

## 3.4 | CD25 is increased in EVs from stage IV CRC-ECM

In addition, CD25, a T lymphocyte marker, was the exclusive marker overexpressed in CRC-ECM-EVs at stage IV in comparison with the respective healthy mucosa (Figure 3a). This increase was also detected in the comparative evaluation with the CRC-ECM-EVs at the stage II-III (Figure 3c), suggesting that the presence of EVs from T lymphocytes expressing CD25 may characterize the stage IV CRC-ECM. To assess the possible link of CD25 expression with the tolerogenic microenvironment in stage IV CRC, we evaluated the presence of CD25 together with FOXP3 and CD4 positive T-cells in sequential slices of CRC biopsies through immunohistochemistry. We confirmed the presence of a significantly higher number of CD25 and FOXP3 positive T-cells in the IV stage compared to the II-III stage CRC (Supplementary Figure 3A-B). The co-expression of CD25 and CD4 in CRC-ECM-EVs was confirmed by single EV analysis using super-resolution microscopy (Supplementary Figure 3C). In addition, CD133, a marker of colon epithelial/stem cells (Peichev et al., 2000), was lower in CRC-ECM-EVs at the stage IV in respect to lower stages (Figure 3c), suggesting a loss of the epithelial phenotype during tumour progression. The ROC curves generated from these data showed a good AUC value with a significant *p*-value for both (Figure 3d and Supplementary Table 3).

3.5 | Signature of ECM-EVs in HC and CRC

Altogether, 16 EV surface antigens were identified as differentially expressed among the extracted EVs in the different tumour stages and decellularized tissue types, which include immune, platelets, or epithelial stemness-related markers (Figure 4a). Principal component analysis (PCA) performed on the significant markers in each comparison showed a specific cluster of HC-ECM-EVs from stage IV CRC in respect to both HC-ECM-EVs and to CRC-ECM-EVs from stage II-III CRC (Figure 4b), suggesting the presence of a subset of ECM-EVs of different origin in healthy mucosa surrounding the stage IV colon tumours.

4 | DISCUSSION

The present study describes for the first time the EV profile within ECM in colon cancer and surrounding mucosa, using decellularized tissues. We assessed the EV surface markers representative of different cell populations possibly present within the tissue
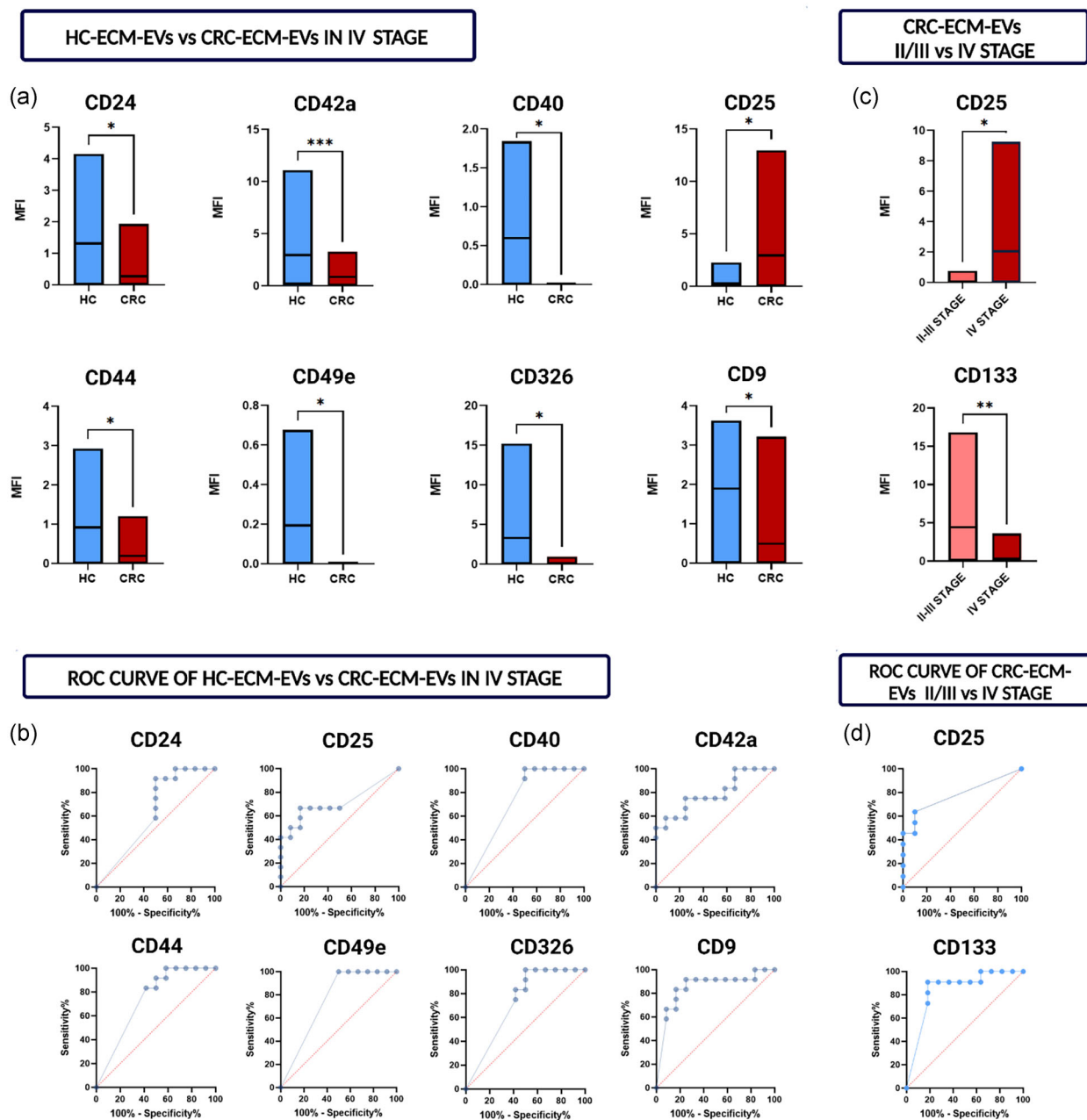
FIGURE 3 Comparison of ECM-EVs from healthy colon mucosa and tumours according to tumour stage. (a-b) Histogram depicting the significantly different expression levels of multiple markers between HC-ECM-EVs and CRC-ECM-EVs in stage IV CRC patients (a), together with corresponding ROC curves (b). (c-d) Histogram of significantly different markers obtained comparing tumour ECM-EVs in the different CRC stages (c) and corresponding ROC curves (d). Multiple T-test was performed: *$p < 0.05$, **$p < 0.01$, ***$p < 0.001$.

or derived from circulation, in order to elucidate the profile of the ECM-EVs. Results highlight a significant modification in the healthy colon mucosa surrounding the primary cancer lesions in stage IV cancer with an increase in EVs expressing immune and platelet markers. In addition, we identified CD25 as a marker specifically and selectively overexpressed in EVs from stage IV tumour tissue in respect to lower tumour stages and normal mucosa.

The ECM is now considered an important reservoir of EVs, that modulates their functions and activity, regulating their stability and destination. In the tumour context, tissue-derived EVs have been isolated either from fresh tissues, including colon carcinoma (Hoshino et al., 2020), leading to the recovery of the EVs present in the different tissue compartments, such as interstitial fluids, matrix, and blood or directly derived from cells. Alternatively, EVs have been isolated by cultured tissues (for instance mouse melanoma (Lunavat et al., 2017), and human renal carcinoma (Jingushi et al., 2018). In detail, Hoshino et al. investigated the proteomic profile of EVs isolated from different types of human tumour specimens, such as lung, pancreatic, and colorectal
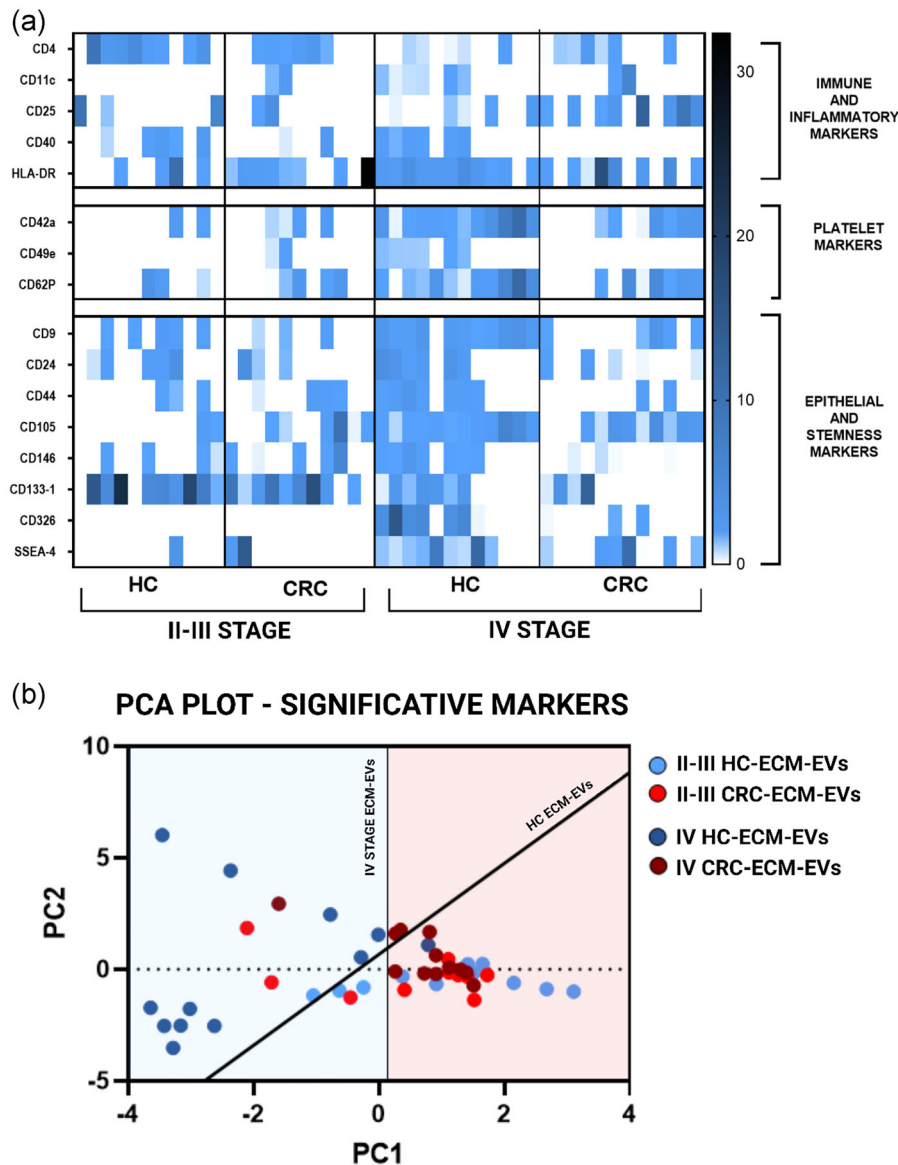
FIGURE 4 Origin and distribution of the significantly different markers in HC- and CRC-ECM-EVs in the different tumour stages. (a) Heatmap and cellular origin of the significantly different markers. (b) PCA performed on the significant markers. The central line highlights the different distribution of IV-stage ECM-EVs, separating HC- versus CRC-ECM-EVs. The diagonal line highlights the different distribution of HC-ECM-EVs, separating the II-III versus IV stage.

cancers (Hoshino et al., 2020). In this manuscript, the authors proposed the use of an EV tissue-related signature able to detect the primary origin of the tumour (Hoshino et al., 2020).

We here selectively focused on ECM-EVs, analyzing decellularized colorectal carcinoma and adjacent non-tumoral mucosa, in order to get insights on the possible role of ECM-EVs entrapped in the tumour and on the modification of the adjacent tissue. Indeed, previous reports indicate that the tumour matrix is modified according to tumour malignancy and by itself may drive tumour progression (Jingushi et al., 2018). Interestingly, a "matrisome protein signature" was previously identified in both primary and metastatic tumour tissues from colorectal cancer patients and was reported to markedly change during tumour progression (Jailkhani et al., 2023). We cannot exclude that ECM-EVs that we analyzed can be part of their analyses.

Several reports indicate that EV cargo influences the tumour microenvironment by activating molecular pathways that differ, in part, from the ones modulated by soluble factors (Webber et al., 2015). Tumour angiogenesis, invasion, and immune escape (Friend et al., 1978; Gabrilovich et al., 2012; Piccoli et al., 2018) are highly modulated by EVs and play a relevant role in tumour progression. In addition, EVs may promote the development of the pre-metastatic niche, infiltrating normal tissue and favouring microenvironment alteration such as angiogenesis and immune tolerance (Ciardiello et al., 2016). We here found that ECM-EVs in tumour tissue mainly expressed immune and platelet markers, together with epithelial cell markers, indicating an

abundance of circulating cell-derived EVs within the ECM. It is conceivable that these ECM-EVs could possibly originate from tissue infiltrating cells, but it cannot be excluded that blood- or lymph-derived EVs may directly extravasate.

Interestingly, in our study, the EV profile in ECM from primary colorectal tumour and healthy mucosa was specifically different only in patients with stage IV colon tumour. We here report a specific profile, characteristic of the stage IV tumour surrounding mucosa, with an increase in epithelial markers, such as CD24 and CD326, and of platelets such as CD42a, and CD49e. The presence of platelet-derived EVs within ECM is indeed of great interest, as tumour-educated platelets are considered an important player in cancer progression and metastasis (Palacios-Acedo et al., 2019). Certainly, they can release pro-angiogenic factors, such as IL-8 and VEGF, as well as immune-modulating factors, such as TGF-beta (Schmied et al., 2021). These results suggest that ECM-EVs are actively involved in creating a supportive microenvironment for tumour progression and for its infiltration in the surrounding tissues. Moreover, many evidences support that the immunological data could better predict patient survival than the histopathological methods in CRC (Angell et al., 2020; Galon et al., 2006; Mlecnik et al., 2011). However, only few data recently demonstrated that the immune microenvironment content in the healthy mucosa of the gastrointestinal tract might provide a picture of the local immune response to cancer, thus giving further information on cancer progression and the recurrence risk, when cancer tissue is no longer available (Kotsafti et al., 2020). Intriguingly, in this line, we demonstrated that ECM-EVs isolated from peritumoral healthy mucosa differ between stage II-III CRC compared to stage IV CRC with platelet and inflammatory cell infiltration, and possibly activation of epithelial cells. These data, once more, suggest how the immune status and relative EV profile on the healthy peri-tumoral colon mucosa is directly related to the tumour stage and could be an interesting field of study as a substitute prognostic biomarker after curative surgery in CRC.

Finally, another relevant finding of our study is the identification of EVs carrying CD25, specifically and selectively found in stage IV tumour ECM in respect to lower tumour stages and normal mucosa. CD25, a component of the IL-2 receptor, is important in T cell proliferation, and it is expressed by both regulatory and effector T cells (Peng et al., 2023). In the present study, CD25 EVs also expressed the CD4 T lymphocyte marker, but we cannot clearly relate them to a regulatory or activated T-cell phenotype. However, several data of the literature suggest that a tolerogenic microenvironment is specifically present in CRC and correlated with a worse prognosis (Bergsland et al., 2022; Liu et al., 2022). Indeed, CD4$^+$CD25$^+$FOXP3$^+$ T regulatory cells are known to be increased both peripherally and at the tumour site in human cancers (Liyanage et al., 2002), as also detected by immunohistochemistry in the present study. These data suggest that CD25-ECM-EVs may rather derive from T regulatory cells.

The study has some limitations. First, the panel of markers used to characterize ECM-EVs is mainly related to blood-circulating EV markers. This allowed the profiling of microenvironmental, and blood infiltrating cell derived EVs within the matrix, but excluded other important tumour and microenvironmental components. Second, the MACSPlex kit provided a semiquantitative analysis of EV markers, and their confirmation and possible co-expression at a single EV level would be important.

In conclusion, the analysis of EVs entrapped in the ECM of normal colon mucosa and colorectal cancer tissue may provide information on the tumour microenvironment and its modulation during tumour progression, and highlight a change in healthy mucosa ECM adjacent to high-stage tumours of possible relevance for tumour spread.

AUTHORS CONTRIBUTION

Sarah Tassinari: Conceptualization; data curation; formal analysis; investigation; methodology; writing—original draft. **Edoardo D'Angelo**: Conceptualization; data curation; investigation; methodology; writing—review and editing. **Federico Caicci**: Formal analysis; methodology. **Cristina Grange**: Formal analysis; investigation; methodology; writing—review and editing. **Jacopo Burrello**: Formal analysis; investigation; supervision. **Matteo Fassan**: Formal analysis; writing—review and editing. **Alessia Brossa**: Formal analysis; methodology; supervision. **Riccardo Quoc Bao**: Data curation; resources. **Gaya Spolverato**: Data curation; resources. **Marco Agostini**: Conceptualization; data curation; funding acquisition; resources; writing—review and editing. **Federica Collino**: Conceptualization; data curation; funding acquisition; supervision; writing—original draft. **Benedetta Bussolati**: Conceptualization; data curation; formal analysis; funding acquisition; investigation; methodology; resources; supervision; writing—original draft.

ACKNOWLEDGEMENTS

CONFLICT OF INTEREST STATEMENT

The authors declare no conflicts of interest.

DATA AVAILABILITY STATEMENT

The datasets generated during and/or analyzed during the current study are available from the corresponding authors upon reasonable request.

ORCID

Alessia Brossa https://orcid.org/0000-0002-5973-5007
Federica Collino https://orcid.org/0000-0002-3619-7701
Benedetta Bussolati https://orcid.org/0000-0002-3663-5134

REFERENCES

Angell, H. K., Bruni, D., Barrett, J. C., Herbst, R., & Galon, J. (2020). The Immunoscore: Colon cancer and beyond. *Clinical Cancer Research: an Official Journal of the American Association for Cancer Research*, 26(2), 332–339. https://doi.org/10.1158/1078-0432.CCR-18-1851

Bergsland, C. H., Jeanmougin, M., Moosavi, S. H., Svindland, A., Bruun, J., Nesbakken, A., Sveen, A., & Lothe, R. A. (2022). Spatial analysis and CD25-expression identify regulatory T cells as predictors of a poor prognosis in colorectal cancer. *Modern Pathology : an Official Journal of the United States and Canadian Academy of Pathology, Inc*, 35(9), 1236–1246. https://doi.org/10.1038/s41379-022-01086-8

Cheng, L., Huang, Z., Zhou, W., Wu, Q., Donnola, S., Liu, J. K., Fang, X., Sloan, A. E., Mao, Y., Lathia, J. D., Min, W., McLendon, R. E., Rich, J. N., & Bao, S. (2013). Glioblastoma stem cells generate vascular pericytes to support vessel function and tumor growth. *Cell*, 153(1), 139–152. https://doi.org/10.1016/j.cell.2013.02.021

Ciardiello, C., Cavallini, L., Spinelli, C., Yang, J., Reis-Sobreiro, M., de Candia, P., Minciacchi, V. R., & Di Vizio, D. (2016). Focus on extracellular vesicles: New frontiers of cell-to-cell communication in cancer. *International Journal of Molecular Sciences*, 17(2), 175. https://doi.org/10.3390/ijms17020175

Cirri, P., & Chiarugi, P. (2011). Cancer associated fibroblasts: The dark side of the coin. *American Journal of Cancer Research*, 1(4), 482–497.

Crescitelli, R., Lässer, C., & Lötvall, J. (2021). Isolation and characterization of extracellular vesicle subpopulations from tissues. *Nature Protocols*, 16(3), 1548–1580. https://doi.org/10.1038/s41596-020-00466-1

d'Alessandro, M., Soccio, P., Bergantini, L., Cameli, P., Scioscia, G., Foschino Barbaro, M. P., Lacedonia, D., & Bargagli, E. (2021). Extracellular vesicle surface signatures in IPF patients: A multiplex bead-based flow cytometry approach. *Cells*, 10(5), 1045. https://doi.org/10.3390/cells10051045

D'Angelo, E., Natarajan, D., Sensi, F., Ajayi, O., Fassan, M., Mammano, E., Pilati, P., Pavan, P., Bresolin, S., Preziosi, M., Miquel, R., Zen, Y., Chokshi, S., Menon, K., Heaton, N., Spolverato, G., Piccoli, M., Williams, R., Urbani, L., & Agostini, M. (2020). Patient-derived scaffolds of colorectal cancer metastases as an organotypic 3D model of the liver metastatic microenvironment. *Cancers*, 12(264), 1–20. https://doi.org/10.3390/cancers12020364

Ekström, K., Crescitelli, R., Pétursson, H. I., Johansson, J., Lässer, C., & Olofsson Bagge, R. (2022). Characterization of surface markers on extracellular vesicles isolated from lymphatic exudate from patients with breast cancer. *BMC cancer*, 22(1), 50. https://doi.org/10.1186/s12885-021-08870-w

Friend, C., Marovitz, W., Henie, G., Henie, W., Tsuei, D., Hirschhorn, K., Holland, J. G., & Cuttner, J. (1978). Observations on cell lines derived from a patient with Hodgkin's disease. *Cancer Research*, 38(8), 2581–2591.

Gabrilovich, D. I., Ostrand-Rosenberg, S., & Bronte, V. (2012). Coordinated regulation of myeloid cells by tumours. *Nature Reviews. Immunology*, 12(4), 253–268. https://doi.org/10.1038/nri3175

Galon, J., Costes, A., Sanchez-Cabo, F., Kirilovsky, A., Mlecnik, B., Lagorce-Pagès, C., Tosolini, M., Camus, M., Berger, A., Wind, P., Zinzindohoué, F., Bruneval, P., Cugnenc, P. H., Trajanoski, Z., Fridman, W. H., & Pagès, F. (2006). Type, density, and location of immune cells within human colorectal tumors predict clinical outcome. *Science (New York, N.Y.)*, 313(5795), 1960–1964. https://doi.org/10.1126/science.1129139

Gebara, N., Scheel, J., Skovronova, R., Grange, C., Marozio, L., Gupta, S., Giorgione, V., Caicci, F., Benedetto, C., Khalil, A., & Bussolati, B. (2022). Single extracellular vesicle analysis in human amniotic fluid shows evidence of phenotype alterations in preeclampsia. *Journal of Extracellular Vesicles*, 11(5), e12217. https://doi.org/10.1002/jev2.12217

Hoshino, A., Kim, H. S., Bojmar, L., Gyan, K. E., Cioffi, M., Hernandez, J., Zambirinis, C. P., Rodrigues, G., Molina, H., Heissel, S., Mark, M. T., Steiner, L., Benito-Martin, A., Lucotti, S., Di Giannatale, A., Offer, K., Nakajima, M., Williams, C., Nogués, L., …, Lyden, D. (2020). Extracellular vesicle and particle biomarkers define multiple human cancers. *Cell*, 182(4), 1044–1061. e18. https://doi.org/10.1016/j.cell.2020.07.009

Huleihel, L., Hussey, G. S., Naranjo, J. D., Zhang, L., Dziki, J. L., Turner, N. J., Stolz, D. B., & Badylak, S. F. (2016). Matrix-bound nanovesicles within ECM bioscaffolds. *Science Advances*, 2(6), e1600502. https://doi.org/10.1126/sciadv.1600502

Jailkhani, N., Clauser, K. R., Mak, H. H., Rickelt, S., Tian, C., Whittaker, C. A., Tanabe, K. K., Purdy, S. R., Carr, S. A., & Hynes, R. O. (2023). Proteomic profiling of extracellular matrix components from patient metastases identifies consistently elevated proteins for developing nanobodies that target primary tumors and metastases. *Cancer Research*, 83(12), 2052–2065. https://doi.org/10.1158/0008-5472.CAN-22-1532

Jingushi, K., Uemura, M., Ohnishi, N., Nakata, W., Fujita, K., Naito, T., Fujii, R., Saichi, N., Nonomura, N., Tsujikawa, K., & Ueda, K. (2018). Extracellular vesicles isolated from human renal cell carcinoma tissues disrupt vascular endothelial cell morphology via azurocidin. *International Journal of Cancer*, 142(3), 607–617. https://doi.org/10.1002/ijc.31080

Kotsafti, A., Scarpa, M., Cavallin, F., Fassan, M., Salmaso, R., Porzionato, A., Saadeh, L., Cagol, M., Alfieri, R., Castoro, C., Rugge, M., Castagliuolo, I., & Scarpa, M. (2020). Immune surveillance activation after neoadjuvant therapy for esophageal adenocarcinoma and complete response. *Oncoimmunology*, 9(1), 1804169. https://doi.org/10.1080/2162402X.2020.1804169

Liu, C., Papukashvili, D., Dong, Y., Wang, X., Hu, X., Yang, N., Cai, J., Xie, F., Rcheulishvili, N., & Wang, P. G. (2022). Identification of tumor antigens and design of mRNA vaccine for colorectal cancer based on the immune subtype. *Frontiers in Cell and Developmental Biology*, 9, 783527. https://doi.org/10.3389/fcell.2021.783527

Liyanage, U. K., Moore, T. T., Joo, H. G., Tanaka, Y., Herrmann, V., Doherty, G., Drebin, J. A., Strasberg, S. M., Eberlein, T. J., Goedegebuure, P. S., & Linehan, D. C. (2002). Prevalence of regulatory T cells is increased in peripheral blood and tumor microenvironment of patients with pancreas or breast adenocarcinoma. *Journal of Immunology (Baltimore, Md: 1950)*, 169(5), 2756–2761. https://doi.org/10.4049/jimmunol.169.5.2756

Lunavat, T. R., Cheng, L., Einarsdottir, B. O., Olofsson Bagge, R., Veppil Muralidharan, S., Sharples, R. A., Lässer, C., Gho, Y. S., Hill, A. F., Nilsson, J. A., & Lötvall, J. (2017). BRAF^{V600} inhibition alters the microRNA cargo in the vesicular secretome of malignant melanoma cells. *Proceedings of the National Academy of Sciences of the United States of America*, 114(29), E5930–E5939. https://doi.org/10.1073/pnas.1705206114

Mlecnik, B., Tosolini, M., Kirilovsky, A., Berger, A., Bindea, G., Meatchi, T., Bruneval, P., Trajanoski, Z., Fridman, W. H., Pagès, F., & Galon, J. (2011). Histopathologic-based prognostic factors of colorectal cancers are associated with the state of the local immune reaction. *Journal of Clinical Oncology: Official Journal of the American Society of Clinical Oncology*, 29(6), 610–618. https://doi.org/10.1200/JCO.2010.30.5425

Palacios-Acedo, A. L., Mège, D., Crescence, L., Dignat-George, F., Dubois, C., & Panicot-Dubois, L. (2019). Platelets, thrombo-inflammation, and cancer: Collaborating with the enemy. *Frontiers in Immunology*, 10, 1805. https://doi.org/10.3389/fimmu.2019.01805

Peichev, M., Naiyer, A. J., Pereira, D., Zhu, Z., Lane, W. J., Williams, M., Oz, M. C., Hicklin, D. J., Witte, L., Moore, M. A., & Rafii, S. (2000). Expression of VEGFR-2 and AC133 by circulating human CD34(+) cells identifies a population of functional endothelial precursors. *Blood*, 95(3), 952–958. https://doi.org/10.1182/blood.v95.3.952.003k27_952_958

Peng, Y., Tao, Y., Zhang, Y., Wang, J., Yang, J., & Wang, Y. (2023). CD25: A potential tumor therapeutic target. *International Journal of Cancer*, *152*(7), 1290–1303. https://doi.org/10.1002/ijc.34281

Piccoli, M., D'Angelo, E., Crotti, S., Sensi, F., Urbani, L., Maghin, E., Burns, A., De Coppi, P., Fassan, M., Rugge, M., Rizzolio, F., Giordano, A., Pilati, P., Mammano, E., Pucciarelli, S., & Agostini, M. (2018). Decellularized colorectal cancer matrix as bioactive microenvironment for in vitro 3D cancer research. *Journal of Cellular Physiology*, *233*(8), 5937–5948. https://doi.org/10.1002/jcp.26403

Rilla, K., Mustonen, A. M., Arasu, U. T., Härkönen, K., Matilainen, J., & Nieminen, P. (2019). Extracellular vesicles are integral and functional components of the extracellular matrix. *Matrix Biology : Journal of the International Society for Matrix Biology*, *75-76*, 201–219. https://doi.org/10.1016/j.matbio.2017.10.003

Schmied, L., Höglund, P., & Meinke, S. (2021). Platelet-mediated protection of cancer cells from immune surveillance—Possible implications for cancer immunotherapy. *Frontiers in Immunology*, *12*, 640578. https://doi.org/10.3389/fimmu.2021.640578

van Niel, G., D'Angelo, G., & Raposo, G. (2018). Shedding light on the cell biology of extracellular vesicles. *Nature Reviews. Molecular Cell Biology*, *19*(4), 213–228. https://doi.org/10.1038/nrm.2017.125

Webber, J. P., Spary, L. K., Sanders, A. J., Chowdhury, R., Jiang, W. G., Steadman, R., Wymant, J., Jones, A. T., Kynaston, H., Mason, M. D., Tabi, Z., & Clayton, A. (2015). Differentiation of tumour-promoting stromal myofibroblasts by cancer exosomes. *Oncogene*, *34*(3), 290–302. https://doi.org/10.1038/onc.2013.560

SUPPORTING INFORMATION

Additional supporting information can be found online in the Supporting Information section at the end of this article.

How to cite this article: Tassinari, S., D'Angelo, E., Caicci, F., Grange, C., Burrello, J., Fassan, M., Brossa, A., Bao, R. Q., Spolverato, G., Agostini, M., Collino, F., & Bussolati, B. (2024). Profile of matrix-entrapped extracellular vesicles of microenvironmental and infiltrating cell origin in decellularized colorectal cancer and adjacent mucosa. *Journal of Extracellular Biology*, *3*, e144. https://doi.org/10.1002/jex2.144